Volume Graphics (2003)
I. Fujishiro, K. Mueller, A. Kaufman (Editors)

A Volume Rendering Approach for Sea Surfaces Taking into Account Second Order Scattering Using Scattering Maps

Kei Iwasaki,[1] Yoshinori Dobashi[2] and Tomoyuki Nishita[1]

[1] Graduate School of Frontier Science, The University of Tokyo, Tokyo, Japan
[2] Graduate School of Engineering, Hokkaido University, Sapporo, Japan

Abstract

We present a fast volume rendering technique for sea surfaces taking into account second order scattering using graphics hardware. To generate realistic images of the sea surfaces, accurate simulation of light transport within water is necessary. In particular, multiple scattering due to particles in the water plays an important role in creating realistic images. In this paper, we introduce the concept of a scattering map for efficient computation of light scattering within water volume. In order to calculate second order scattering of light, we slice the water volume into virtual horizontal planes and calculate the radiance from second order scattering of light at sampling points on these planes. The radiance on the virtual planes can be treated as a texture map. This makes it possible to accelerate the computation using graphics hardware.

Categories and Subject Descriptors (according to ACM CCS): I.3.7 [Computer Graphics]: Three-Dimensional Graphics and Realism

1. Introduction

Rendering participating media, such as water, smoke and clouds, is one of the challenging tasks in the research field of volume rendering. This paper focuses on the rendering of the sea as the participating medium. The color of the sea is determined by the reflection of light from the sun and the sky, scattered light due to small particles such as water molecules, and light reflected from the bottom of the sea. The scattered light and the light reflected from the bottom are attenuated by the particles in the water before reaching the viewpoint. In these optical phenomena, the physical simulation of scattering of light is necessary in order to create realistic images. This implies that multiple scattering of light must be taken into account for rendering the sea. To take multiple scattering into account, one must solve the rendering equation, which expresses an energy equilibrium for the light scattered between the particles. In optical oceanography, a radiative transfer equation that is modified version of the volume rendering equation is used. Several methods for the clouds and the atmospheric scattering have been developed to solve this problem [11, 15, 20, 6]. Although these methods make it possible to create realistic images of natural scenes, the computational cost is large.

In this paper, we propose an efficient method for computing second order scattering by making use of graphics hardware. In the methods previously developed, images are created by generating a number of sample points on the viewing ray to compute the total radiance scattered towards the viewpoint. In the proposed method, virtual surfaces, which we call sampling planes, are generated. We calculate the scattered radiance at points on the sampling planes. The radiance distribution on each sampling plane is stored as a texture, which we call a scattering map. We compute the scattering maps by using hardware color blending functions and an accumulation buffer. Then we accumulate values of the scattering maps into the accumulation buffer. The color distribution of the water surface is obtained by mapping the accumulated values of the scattering maps onto the water surface and adding the other two components: the reflected light from the sun and the sky and the reflected light from the bottom. Previous methods computed light scattering point by point, whereas our method does this surface by surface. This means that the method is well suited for hardware-acceleration since the basic primitives of graphics hardware are polygons.

2. Previous Work

There are many methods for modeling and rendering the sea. Peachey presented a method that can simulate breaking waves and wave refractions near the shore [16]. Fournier and Reeves proposed a method for displaying coastal scenes by using Gerstner's wave model [3]. Ts'o and Basky demonstrated wave refraction and represented waves by using B-splines [23]. In 2000, Gonzato and Saëc displayed the diffraction of waves [4]. Tessendorf introduced a statistical wave model that represents waves as the synthesis of sine and cosine waves by using Fast Fourier Transformation [22]. These methods mainly describe the modeling of sea waves.

Techniques that simulate the light transport in participating media have been proposed. Kajiya et al. used a spherical harmonics approach [9]. However, a large number of spherical harmonics are required to obtain an accurate solution. Rushmeier et al. developed a zonal method by extending the radiosity method to take into account the participating medium [19]. In this method, a simulation space is discretized into voxel elements and the state of the energy equilibrium between the voxels is obtained by solving simultaneous linear equations. The method, however, cannot handle an anisotropic phase function of particles. Max improved this method in order to handle the phase function by using direction bins [11]. This method requires many bins, resulting in an increase in the computation time. Blasi used the Monte Carlo method for determining the scattering direction of photons, but he did not calculate the scattered component in the viewing ray. Therefore, this method cannot be considered to be one that takes into account the anisotropic phase function [1]. Max proposed a method for calculating multiple scattering from vegetation [12]. Methods for subsurface scattering are proposed for rendering skin, leaves, and objects covered by dust [5, 17, 7]. These methods, however, do not deal with rendering of the sea.

As to the simulation of light transport within the water body, the radiative transfer equation has to be solved. Kaneda et al. displayed a realistic water surface by solving the ratiative transfer equation [10]. Nishita et al. modified Kaneda's method in order to take into account atmospheric scattering, and rendered images of the sea viewed from a space shuttle [14]. In their papers, only single order scattering is considered. Furthermore, these methods have the limitation that the depth is constant. Premoze and Ashikhmin simplified the radiative transfer equation and demonstrated the colors of the water under various conditions [18]. In the simplified equation, they did not attempt to obtain an analytical solution of the integration term of scattered light in the radiative transfer equation. They estimated the total radiance of the scattered light by using empirical equations and experimental data. Therefore their method lacks generality. Mobley developed an analytical solution for the radiative transfer equation [13].

This method, however, requires a time-consuming precalculation to solve the equation, and assumes that the bottom of the sea is flat. The proposed method takes into account second order scattering by using scattering maps. Moreover, our method can compute second order scattering of light even if the bottom of the sea is not uniform.

$L(z,\theta,\phi,\lambda)$	radiance of wavelength λ
$L^{(i)}(z,\theta,\phi,\lambda)$	radiance of ith order scattered light
$\beta(\alpha,\lambda)$	volume scattering function
$a(\lambda)$	absorption coefficient
$b(\lambda)$	scattering coefficient
$c(\lambda)$	extinction coefficient ($c(\lambda) = a(\lambda) + b(\lambda)$)
$\omega_0(\lambda)$	albedo ($\omega_0(\lambda) = b(\lambda)/c(\lambda)$)
$c_f(\lambda)$	forward scattering coefficient
n	refraction index of water

Table 1: Definitions of terms and symbols.

3. Radiative Transfer Equation

In rendering the sea, it is very important to simulate the behavior of light on the water surface and within the water. The color of the sea is calculated by the reflection of light from the sun and the sky, scattered light within the water and light reflected from the bottom of the sea. We assume that the density distribution of water particles within water is uniform. For calculating the radiance of light scattered within the water and light reflected at the bottom of the sea, the water surface is assumed to be flat.

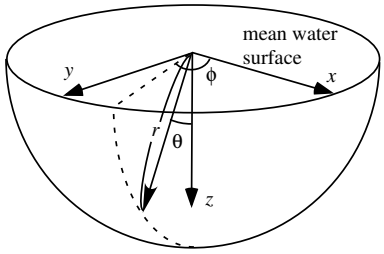

Figure 1: *Definitions of polar coordinates* (θ,ϕ).

Since reflection and refraction of light at the water surface have been discussed in previous methods, we would like to focus attention on light transported from the water volume. The radiance L at depth z towards direction (θ,ϕ) (see Fig. 1) is calculated from the radiative transfer equation (the sym-

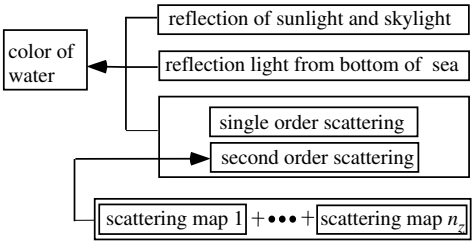

Figure 2: *Calculation of color of sea (n_z is number of sampling planes).*

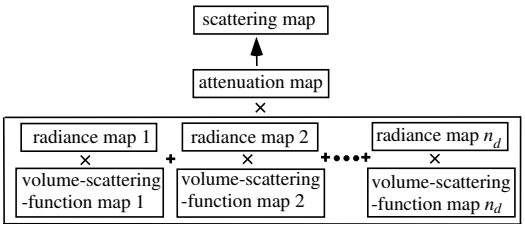

Figure 3: *Calculation of scattering map (n_d is number of sampling directions).*

bols used in this paper are defined in Table 1).

$$\frac{dL(z,\theta,\phi,\lambda)}{dr} = -c(\lambda)L(z,\theta,\phi,\lambda) + \int_0^{2\pi}\int_0^{\pi}\beta(\alpha,\lambda)L(z,\theta',\phi',\lambda)\sin\theta' d\theta' d\phi', \quad (1)$$

where θ' and ϕ' are the integration variables. In Eq. (1), the first term represents the attenuation of light, and the second term is the component of scattered light. dr is a differential length of optical path expressed by $dr = dz/\cos\theta$, and α is the angle between the incoming light direction and the outgoing light direction. $\beta(\alpha,\lambda)$ is calculated by the following equation:

$$\beta(\alpha,\lambda) = \frac{(1-g^2)b(\lambda)}{4\pi(1+g^2-2g\cos\alpha)^{3/2}}, \quad (2)$$

where g is the Henyey-Greenstein parameter. $\beta(\alpha,\lambda)$ satisfies the following equation:

$$\int_{\Omega_{4\pi}}\beta(\alpha,\lambda)d\Omega = 2\pi\int_0^{\pi}\beta(\alpha,\lambda)\sin\alpha d\alpha = b(\lambda) \quad (3)$$

Eq. (1) can be rewritten by integrating along the optical path. The radiance L is expressed by the following equation.

$$L(z,\theta,\phi,\lambda) = \int_0^z \exp(-c(\lambda)\frac{z'}{\cos\theta}) \times \int_0^{2\pi}\int_0^{\pi}\beta(\alpha,\lambda)L(z',\theta',\phi',\lambda)\sin\theta' d\theta' d\phi' \frac{dz'}{\cos\theta}, \quad (4)$$

where z' is the integration variable. However, this equation cannot be solved directly, since the quantity L itself is involved in the integration term of the equation. Therefore, we choose an approach that uses the Neumann series. The radiance $L(z,\theta,\phi,\lambda)$ is expressed by the sum of each radiance $L^{(i)}(z,\theta,\phi,\lambda)$ that represents the ith order of scattered light. The proposed method employs the analytical solution of $L^{(1)}(z,\theta,\phi,\lambda)$. We can calculate the second order scattering of light $L^{(2)}(z,\theta,\phi,\lambda)$, since the effect of second order scattering is often stronger than that of a single scattering process [21]. In addition, we accelerate the computation of second order scattering by using graphics hardware.

4. Overview of Our Method

We calculate the color of the sea by using three components, that is, the reflected light from the sun and the sky, scattered light within water and transmitted light reflected from the bottom of the sea (see Fig. 2). For the scattered light, single and second order scattering are taken into account. The radiance due to single scattering can be calculated analytically [14]. On the other hand, the radiance due to second order scattering reaching the viewpoint is computed by using numerical integration methods since analytical solutions are almost impossible. In our method, sampling planes are generated for the numerical calculation. Then we calculate the radiance distribution on each sampling plane and store it as a texture. We call this texture map a scattering map. The scattering maps store the radiance due to second order scattering towards the viewpoint.

The scattering maps are obtained as follows (see Fig. 3). The radiance due to second order scattering reaching the viewpoint is calculated by multiplying two factors. These two factors are the radiance due to second order scattering at a point on the sampling plane, and the attenuation ratio between the point and the viewpoint. The radiance due to second order scattering towards the viewpoint is computed by the integrating the product of the incident radiance due to single scattering towards a point on the sampling plane and value of the volume scattering function. To create the scattering map, we prepare three maps: the radiance map, the volume-scattering-function map and the attenuation map. The radiance map stores the incident radiance due to single order scattering at points on the sampling planes. The volume-scattering-function map stores a value of the volume scattering function for each phase angle, and the attenuation map stores the attenuation ratios between points on the sampling planes and the viewpoint. As a result, the scattering map is generated by using three maps. The radiance due to second order scattering is calculated by accumulating values of the scattering maps into the accumulation buffer.

The reflected light from the sun and the sky is computed by using the reflection mapping technique. That is, a texture that stores the intensities of the sun and the sky is mapped onto the water surface.

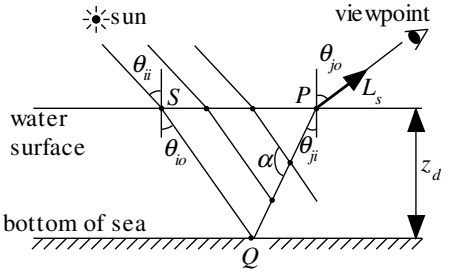

(a) computing single scattering

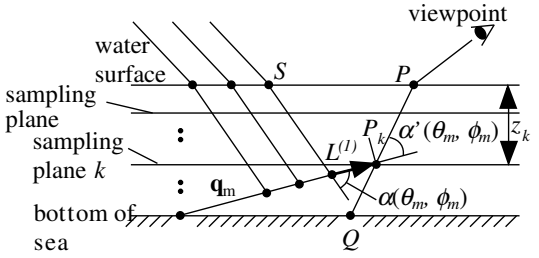

(b) computing second order scattering

Figure 4: *Calculation of scattered light.*

5. Calculation of the Color of the Sea

Suspensions within water are the main cause of light scattering within water. This is the reason why the color of water is bluish. We first propose a calculation method for the color of the sea by assuming that the depth of the water is constant. In regions far from the seashore, this is a reasonable assumption and here multiple scattering strongly influences the color of the sea. In this case, there is an efficient way to compute the multiple scattering. On the other hand, for regions near the seashore, the method is extended to handling the case where the depth is not constant. In the shallow regions, multiple scattering is less important and therefore the multiple scattering is evaluated approximately by generating discrete sampling points.

5.1. Single Scattering

An analytical expression has already been obtained to describe the color of water taking into account single scattering [14]. As shown in Fig.4 (a), let S be an intersection point between the water surface with the sunlight, let Q be an intersection point between the bottom of the sea and the refracted sunlight, and let P be an intersection point of the water surface with the viewing ray. The sum of the radiance L_s of the light scattered at points on path QP is given by the following equation.

$$L_s(z_d,\theta_{ii},\theta_{io},\lambda) = \frac{L_{sun}(\lambda)T_i(\theta_{ii},\theta_{io})T_o(\theta_{jo},\theta_{ji})\beta(\alpha,\lambda)}{(\cos\theta_{io}+\cos\theta_{ji})c(\lambda)(1-\omega_0(\lambda)c_f(\lambda))} \quad (5)$$
$$\times(1-\exp(-z_d c(\lambda)(1-\omega_0(\lambda)c_f(\lambda))(\sec\theta_{ji}+\sec\theta_{io})),$$

where λ is the wavelength, at RGB in this paper, z_d is the depth of the sea, L_{sun} is the irradiance of the sun, T_i and T_o are the transmission ratios at points S and P, respectively, θ_{ii} and θ_{io} are respectively the incidence angle and refraction angle of the sunlight, and θ_{jo} and θ_{ji} are respectively the incidence angle and refraction angle of the viewing ray (see Fig. 4(a)). ω_0 is the albedo and $c_f(\lambda)$ is the forward scattering coefficient (see Table. 1). $c_f(\lambda)$ is computed by the following equation, $2\pi\int_0^{\pi/2}\beta(\alpha,\lambda)\sin\alpha d\alpha$. Snell's law allows us to compute the refraction angles θ_{io} and θ_{ji} by the incident angles θ_{ii} and θ_{jo}, respectively. Therefore, the parts of Eq. (5) except $\beta(\alpha,\lambda)$ can be regarded as the function of θ_{jo},θ_{ii} and z_d. When the depth z_d is constant and the direction of the sun is fixed (i.e. the angle θ_{ii} is fixed), those parts are the function of θ_{jo}. Therefore, for efficient computation, we create a look-up table that stores their values at each angle θ_{jo}. This table is updated when the sun direction is changed.

5.2. Second Order Scattering

We employ a numerical integration method to calculate the second order scattering. As shown in Fig. 4(b), n_z sampling planes are generated for the integration. Let P_k be a point on the viewing ray, let $L^{(1)}(z_k,\theta,\phi,\lambda)$ be the incident radiance at point P_k from direction (θ,ϕ), and let z_k be the depth of point P_k. $L^{(1)}(z_k,\theta,\phi,\lambda)$ is the sum of the scattered radiance at points on a sampling ray q_m (see Fig. 4(b)). Then the radiance $L^{(2)}$ at P_k of the light due to second order scattering is obtained from the following equation:

$$L^{(2)}(z_k,\lambda)=\int_0^{2\pi}\int_0^{\pi}\beta(\alpha',\lambda)G(z_k)L^{(1)}(z_k,\theta,\phi,\lambda)\sin\theta d\theta d\phi, \quad (6)$$

where G is the attenuation ratio between point P_k and the water surface, and is expressed by $\exp(-c(\lambda)z_k\sec\theta_{ji})$. An analytical solution for $L^{(1)}(z_k,\theta,\phi,\lambda)$ is expressed by the following equation.

$$L^{(1)}(z_k,\theta,\phi,\lambda) = L^*(\theta,\phi,\lambda)[\exp(-c(\lambda)z_k\sec\theta_{io}) \quad (7)$$
$$-\exp(-c(\lambda)z_k\sec\theta)],\ (0<\theta\le\pi/2)$$
$$L^{(1)}(z_k,\theta,\phi,\lambda) = L^*(\theta,\phi,\lambda)[\exp(-c(\lambda)z_k\sec\theta_{io})$$
$$-\exp(-c(\lambda)(z_d\sec\theta_{io}-(z_d-z_k)\sec\theta))],\ (\pi/2<\theta<\pi)$$
$$L^*(\theta,\phi,\lambda) = \frac{L_{sun}(\lambda)T(\theta_{ii},\theta_{io})\beta(\alpha(\theta,\phi),\lambda)}{c(\lambda)(1-\sec\theta_{io}\cos\theta)}.$$

To compute Eq. (6), we discretize θ and ϕ. Eq. (6) can be rewritten as follows.

$$L^{(2)}(z_k,\lambda) = G(z_k)\sum_{m=1}^{n_d}\beta(\alpha'(\theta_m,\phi_m),\lambda) \quad (8)$$
$$\times\ L^{(1)}(z_k,\theta_m,\phi_m,\lambda)\sin\theta_m\Delta\theta\Delta\phi,$$

where $\Delta\theta$ and $\Delta\phi$ are the sampling angles, (θ_m,ϕ_m) is the mth sampling direction and n_d is the number of sampling directions.

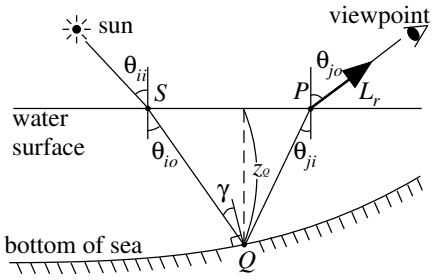

Figure 5: *Calculation of light reflected from bottom of sea.*

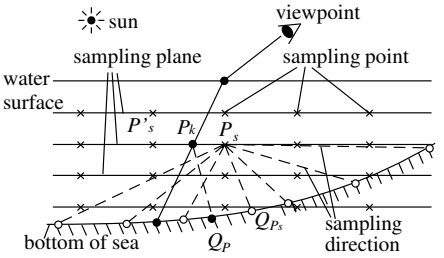

Figure 6: *Sampling planes and sampling points.*

The scattering map for each sampling plane is generated by calculating Eq. (8) for n_d sampling directions (see Fig. 3). We create the scattering map by using three maps: the radiance map, the volume-scattering-function map and the attenuation map. The radiance map is generated by calculating Eq. (7). The radiance map is a three dimensional texture whose parameters are z, θ, and ϕ. If the sun's position is changed, only the radiance map has to be updated. The volume-scattering-function map is generated by calculating $\beta(\alpha'(\theta_m, \phi_m), \lambda)$ for each phase angle at point P_k. The phase angle $\alpha'(\theta_m, \phi_m)$ is the angle between the incoming light direction (θ_m, ϕ_m) and the outgoing direction towards the viewpoint (see Fig. 4(b)). The volume-scattering-function map is a one dimensional texture whose parameter is the phase angle α.

The attenuation map is created by calculating $G(z_k)$. The attenuation map is a one dimensional texture whose parameter is the length $z_k \sec\theta_{ji}$. We multiply the radiance map by the volume-scattering-function map for n_d directions and accumulate the values of the multiplied two maps into the accumulation buffer. Then the scattering map is obtained by multiplying the attenuation map by the accumulated values. The multiplication is accelerated by using color blending functions.

The radiance due to second order scattering is obtained by accumulating the values of the scattering maps into the accumulation buffer. The color of water is obtained by summing the radiance due to the scattering, the reflected radiance from the bottom of the sea and the reflected radiance of the sky and the sun at the water surface.

5.3. Calculation of Light Reflected from the Bottom

This subsection describes the calculation method for the light reflected at the bottom of the sea. The reflected light is attenuated due to water particles before reaching the viewpoint. Since we assume that the water surface is flat, the refracted sunlight is parallel. Therefore, the radiance $L'_{sun}(\lambda)$ of the sunlight reaching point Q is calculated by using depth z_d in Fig. 4(a). The attenuation ratio between PQ is expressed by $\exp(-c(\lambda)z_d \sec\theta_{ji})$. Radiance of the reflected light, L_r, is calculated from the following equation.

$$L_r(z_d) = T_o(\theta_{jo}, \theta_{ji}) L'_{sun}(\lambda) K_d \cos\gamma \exp(-c(\lambda) z_d \sec\theta_{ji}), \quad (9)$$

where K_d is the reflectance of the bottom of the sea, γ is the angle between the refracted sunlight and the normal of point Q (see Fig. 5).

5.4. Calculation Method for the Non-uniform Bottom

Let us now discuss the calculation method in the case that the depth of the sea is not constant. We represent the bottom of the sea as a height field. We first describe the calculation method for reflected light from the bottom. In order to calculate the light reflected from the bottom reaching the viewpoint, it is necessary to calculate the depth of point Q, which is the intersection point between the refracted viewing ray at P and the bottom of the sea. Then we substitute depth z_d of Eq. (9) for depth z_Q (see Fig. 5). The calculation method for the single scattering light is almost the same as the one for the reflected light. That is, the radiance L_S is calculated by substituting z_d of Eq. (5) for depth z_Q (see Fig. 5).

The calculation method for the second order scattering, however, is not so simple. The total radiance reaching point P_k from direction (θ, ϕ) is the integration of the radiance along $Q_P P_k$ (see Fig. 6). Therefore, we have to calculate the intersection points between all the sampling rays and the bottom of sea. However, this requires a large amount of computational cost. In order to reduce the computational time, we pre-calculate the intersection points and store their depth in advance. The depths are used for computing the incident radiance at P_k by using Eq. (7). To achieve this, we generate sampling points P_s on each sampling plane as shown in Fig. 6. Then we calculate the intersection point Q_{P_s} between the bottom of the sea and the sampling ray in the direction of (θ_m, ϕ_m) from point P_s, and store the depth of Q_{P_s} in a table. The depths for all the sampling directions are calculated in advance and stored in the table. Using this table, the incident radiance at point P_k is obtained efficiently. That is, for each sampling direction (θ_m, ϕ_m), the depth value is interpolated by using the corresponding depths of points P_s and P'_s stored in the table. Then the incident radiance from the direction (θ_m, ϕ_m) is computed by using Eq. (7).

6. Examples

Fig. 9 shows examples of natural scenes. In Fig. 9(a), only single scattering of light is taken into account, whilst second order scattering is taken into account in Fig. 9(b). As shown in Figs. 9(a) and (b), the color of the sea becomes more bluish when taking into account second order scattering. This fact indicates that multiple scattering is important for the sea. Fig. 10 shows examples of a natural scene in a tropical region. These figures are also rendered taking into account second order scattering. The color of the tropical sea is simulated by changing the extinction coefficient of the water particles. Clouds in these images are rendered by using Dobashi's method [2]. In Fig. 9(b), clouds are rendered taking into account multiple scattering.

Fig. 11 shows examples of the seashore. The bottom of the sea is not flat in this case. We can observe color variations of the water due to the depths of the water bottom. In the shallow regions, the color of the water becomes brighter since the influence of the bottom is significant. Fig. 11(b) shows the comparison under different conditions. The multiple scattering is taken into account in the top row and only the single scattering is taken into account in the bottom row. The depths of the water bottom in images on the right are deeper than those on the left. The maximum depths are 7.9[m] in the left images and 39.9[m] in the right images, respectively. The color of the bottom is significant when the water is shallow. The multiple scattering does not seem to be important in this case. It becomes important when the bottom becomes deeper. When the bottom is deep enough, the color of the bottom becomes less important and the variations of the depths can be ignored. This implies that the assumption in our method is valid, that is, the bottom of the water can be assumed to be flat in the deeper regions. As shown in these images, the proposed method can create very realistic images when taking into account second order scattering.

Water waves are generated by using the statistical wave model proposed by Tessendorf [22]. We obtained the values such as scattering coefficient and extinction coefficient from the book [13]. A desktop PC with a Pentium III (1GHz) processor is used to create these images. This machine has an Intence3D Wildcat4110 as the graphics board. The rendering times for Figs. 9 and 10 are about 0.5 seconds. The rendering time for Fig. 11 is about 2 seconds since the bottom of the sea is not uniform in this figure. The precomputation time for creating the textures is about 1.5 seconds. The precomputation time for the look-up tables of depths for non-uniform depth is about 30 seconds. The computational time for second order scattering in Fig. 9(b) using hardware is about 0.14 seconds. The computational time for second order scattering using software is about 30 seconds. That is, the method using hardware is 200 times faster than the method using software. In our experiment, we have rendered the sea very efficiently.

6.1. Estimation of Sampling Numbers

The proposed method uses sampling planes and calculates the radiance due to second order scattering numerically for different sampling directions. Therefore, the accuracy of the radiance due to second order scattering depends on the number of sampling planes and sampling direction. We determined the optimal values for these numbers experimentally. Let $L_v^{(2)}(n_z)$ be the radiance of second order scattered light towards the viewpoint and n_z be the number of sampling planes. We calculate the maximum difference between $L_v^{(2)}(n_z)$ and $L_v^{(2)}(n_z+1)$. The optimal value is determined when the maximum difference becomes smaller than a threshold ε (we choose ε to be $0.0039(\approx 1/255)$ since most graphics hardware stores the RGB values for each pixel with 8bit precision). Fig. 7 shows the relationship between the number of sampling planes n_z and the maximum difference between $L_v^{(2)}(n_z)$ and $L_v^{(2)}(n_z+1)$. n_d can be determined in the same way (see Fig. 8). The number of sampling planes is 12 since the difference is less than ε as shown in Fig. 7. The number of sampling directions is 128. In our experiment, the resolution of the scattering maps is 32×32 in the case that the bottom is uniform. That is, the radiance of 32×32 points on each sample plane are calculated by using scattering maps. In the case that the bottom is not uniform, we used the resolution of the scattering map as 64×64.

7. Conclusion and Future Work

We have proposed a new method for rendering the sea taking into account second order scattering. We have introduced the concept of scattering maps for efficient computation by using graphics hardware. The conclusions that we have reached regarding the application of our method are as follows.

1. Second order scattering is calculated by compositing the scattering maps.
2. Graphics hardware functions such as an accumulation buffer and texture mapping are used for the acceleration of the computation.
3. The proposed method can evaluate second order scattering efficiently even if the bottom of the sea is not constant.

Our results indicate that multiple scattering is important for an accurate rendering of the sea.

In our future work, we want to take into account higher order scattering. The diffusion method has been recently introduced for rendering [7, 8]. Therefore we want to render the sea by using the diffusion approximation and accelerate the computation by using graphics hardware. Moreover, we want to render foam and spray since these effects increase realism in the images of the sea.

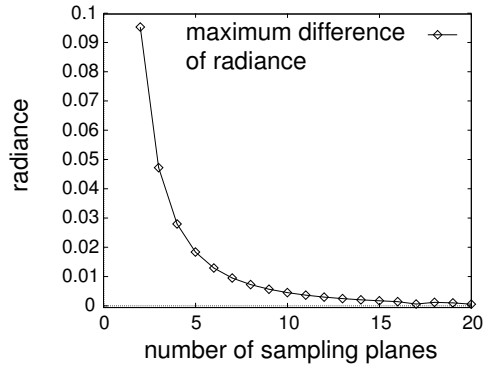

Figure 7: *Relationship between maximum difference of radiance and numbers of sampling planes.*

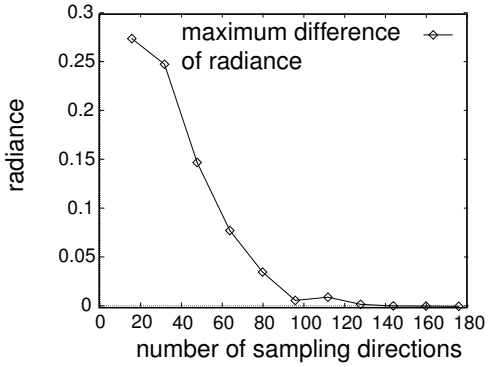

Figure 8: *Relationship between maximum difference of radiance and numbers of sampling directions*

References

1. P. Blasi, B. Le. Saëc, C. Schlick, "A Rendering Algorithm for Discrete Volume Density Object," *Eurographics'93,* 1993, pp.201-210.
2. Y. Dobashi, K. Kaneda, H. Yamashita, T. Okita, T. Nishita, "A Simple, Efficient Method for Realistic Animation of Clouds," *Proc. SIGGRAPH2000,* 2000, pp.19-28.
3. A. Fournier, W.T. Reeves, "A Simple Model of Ocean Waves," *Proc. SIGGRAPH'86,* 1986, pp.75-84.
4. J.C. Gonzato, B.Le. Saëc, "On Modeling and Rendering Ocean Scenes," *Visualization and Computer Animation,* 2000, Vol. 11, No. 1, pp.27-37.
5. P. Hanrahan, W. Krueger, "Reflection from Layered Surfaces due to Subsurface Scattering," *SIGGRAPH'93,* 1993, pp.165-174.
6. H. W. Jensen, P. H. Christensen, "Efficient Simulation of Light Transport in Scenes with Participating Media using Photon Maps," *Proc. SIGGRAPH'98,* 1998, pp.311-320.
7. H. W. Jensen, S. Marschner, M. Levoy, P. H. Christensen, "A Practical Model for Subsurface Light Transport," *Proc. SIGGRAPH'2001,* 2001, pp.511-518.
8. H. W. Jensen, J. Buhler, "A Rapid Hierarchical Rendering Technique for Translucent Materials," *Proc. SIGGRAPH'2002,* 2003, pp.576-581.
9. J. T. Kajiya, B. P. V. Herzen, "Ray Tracing Volume Densities," *Computer Graphics,* 1984, Vol. 18, No. 3, pp.165-174.
10. K. Kaneda, G. Yuan, Y. Tomoda, M. Baba, E. Nakamae, T. Nishita, "Realistic Visual Simulation of Water Surfaces Taking into Account Radiative Transfer," *Proc. CAD/Graphics'91,* 1991, pp.25-30.
11. N. Max, "Efficient Light Propagation for Multiple Anisotropic Volume Scattering," *Proc. the Fifth Eurographics Workshop on Rendering,* 1994, pp.87-104.
12. N. Max, C. Mobley, B. Keating, E-H. Wu, "Plane-Parallel Radiance Transport for Global Illumination in Vegetation," *Proc. the Eighth Eurographics Workshop on Rendering,* 1997, pp.239-250.
13. C.D. Mobley, "Light and Water. Radiative Transfer in Natural Waters," *Academic Press,* 1994.
14. T. Nishita, T. Shirai, K. Tadamura, E. Nakamae, "Display of The Earth Taking into account Atmospheric Scattering," *Proc. SIGGRAPH'93,* 1993, pp.175-182.
15. T. Nishita, Y. Dobashi, E. Nakamae, "Display of Clouds Taking into Account Multiple Anisotropic Scattering and Sky Light," *Proc. SIGGRAPH'96,* 1996, pp.379-386.
16. D. Peachey, "Modeling Waves and Surf," *Proc. SIGGRAPH'86,* 1986, pp.65-74.
17. M. Pharr, P. Hanrahan, "Monte Carlo Evaluation of Non-Linear Scattering Equations for Subsurface Reflection," *Proc. SIGGRAPH2000,* 2000, pp.75-84.
18. S. Premoze and M. Ashikhmin, "Rendering Natural Waters," *Proc. Pacific Graphics 2000,* 2000, pp.23-30.
19. H. E. Rushmeier, K. E. Torrance, "The Zonal Method for Calculating Light Intensities in The Presence of a Participating Medium," *Computer Graphics,* Vol. 21, No. 4, 1987, pp.293-302.
20. J. Stam, E. Fiume, "Depicting Fire and Other Gaseous Phenomena Using Diffusion Processes," *Proc. SIGGRAPH'95,* 1995, pp.129-136.
21. Y. Sugimori, W. Sakamoto, "Marine Enviromental Optics,"(in Japanese) *Tokai University Press,* 1985.
22. J. Tessendorf, "Simulating Ocean Water," *Course Note #25 of SIGGRAPH'99,* 1999, pp.1-18.
23. P.Y. Ts'o, B.A. Barsky, "Modeling and Rendering Waves: Wave-Tracing Using Beta-Splines and Reflective and Refractive Texture Mapping," *ACM Trans. on Graphics,* 1987, Vol. 6, No. 3, pp.191-214.

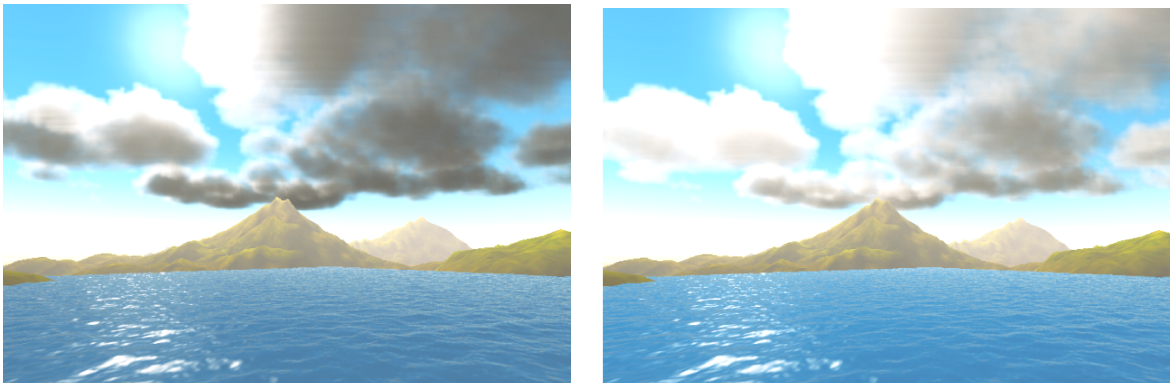

(a) single scattering. (b) multiple scattering.

Figure 9: *Examples of natural scenes.*

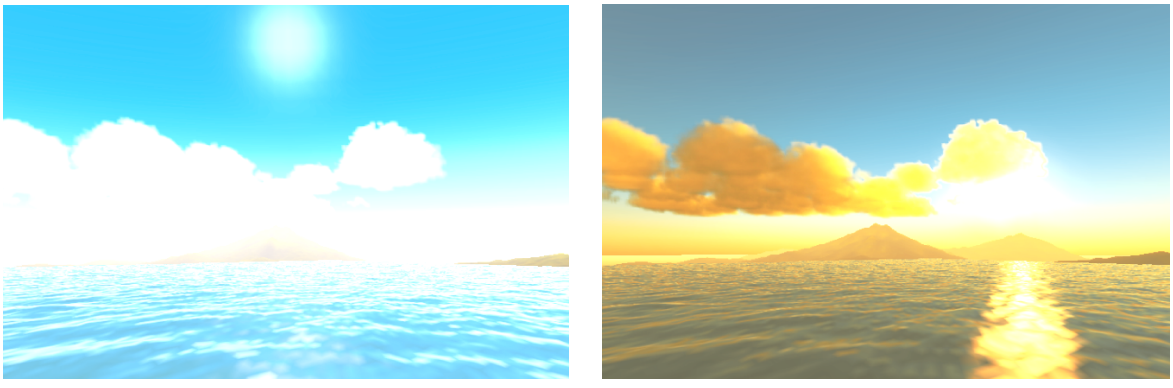

(a) daytime. (b) sunset scene.

Figure 10: *Examples of natural scenes in tropical regions.*

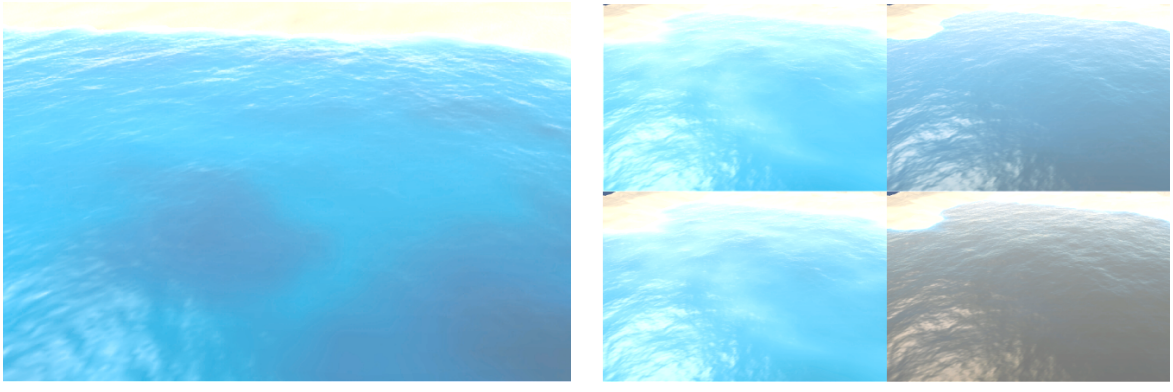

(a) seashore in daytime.

(b) comparison under different conditions
(top left: shallow, multiple scattering,
top right: deep, multiple scattering,
bottom left: shallow, single scattering,
bottom right: deep, single scattering).

Figure 11: *Examples of the seashore.*

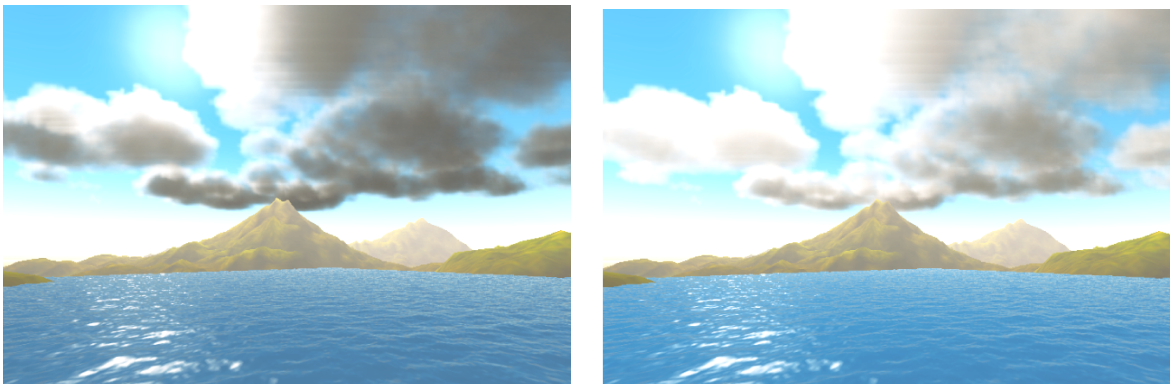

(a) single scattering. (b) multiple scattering.

Figure 9: *Examples of natural scenes.*

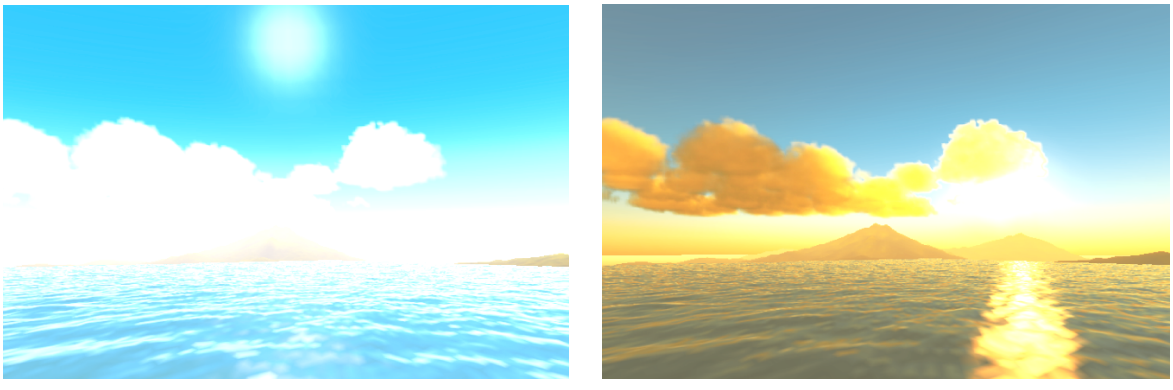

(a) daytime. (b) sunset scene.

Figure 10: *Examples of natural scenes in tropical regions.*

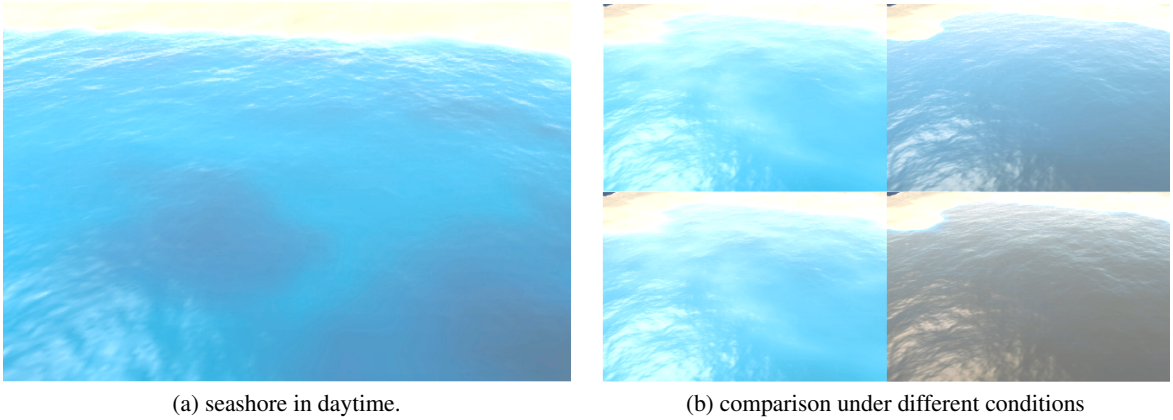

(a) seashore in daytime.

(b) comparison under different conditions
(top left: shallow, multiple scattering,
top right: deep, multiple scattering,
bottom left: shallow, single scattering,
bottom right: deep, single scattering).

Figure 11: *Examples of the seashore.*